

Photonic Generation of Linearly Chirped Microwave Waveforms With Tunable Parameters

Hao Zhang¹, Fangzheng Zhang¹, *Senior Member, IEEE*, Shilong Pan¹, *Senior Member, IEEE*,
Xingwei Ye¹, *Student Member, IEEE*, Shifeng Liu¹, and Hao Chen

Abstract—We propose a linearly chirped microwave waveform (LCMW) generation scheme applying a stimulated Brillouin scattering (SBS)-based Fourier domain mode locked (FDML) optoelectronic oscillator (OEO). In this system, SBS-induced phase-modulation-to-intensity-modulation-conversion is adopted to build a microwave photonic filter, of which the pass-band can be rapidly tuned by adopting a high-order frequency sweeping modulation sideband as the optical carrier. Thanks to the frequency multiplication capability and the fast mode selection with a very narrow pass band, the proposed system can generate broadband LCMWs with a good frequency modulation linearity. Besides, the bandwidth, central frequency, duty cycle and repetition rate of the LCMWs can be easily adjusted to satisfy different radar applications. A proof-of-concept experiment is carried out. The results can soundly verify the feasibility as well as the flexibility of the proposed LCMW generation system.

Index Terms—Linearly chirped microwave waveform, microwave photonics, stimulated Brillouin scattering, optoelectronic oscillator, Fourier domain mode locking.

I. INTRODUCTION

LINEARLY chirped microwave waveform (LCMW) has wide applications in radar systems [1]–[3]. Traditionally, LCMWs are produced by electrical systems such as a direct digital synthesizer (DDS) or a voltage-controlled oscillator (VCO). However, the signal bandwidth is usually constrained by the electronic bottleneck, resulting in a limited range resolution of the radar [4]. To address this, various microwave photonic methods have been proposed to generate broadband LCMWs, including the temporal pulse shaping method [5], the spectral shaping with frequency-to-time mapping method [6], [7], the optical laser injection method [8], and the photonic frequency multiplication method [9], etc. Recently, Fourier domain mode locked (FDML) optoelectronic oscillator (OEO) has been demonstrated to generate LCMWs [10]–[13]. An OEO is often used to generate single-tone RF signals with significantly superior short-time stabilities over electrical signal generators [14]. To generate broadband LCMWs, the OEO oscillation frequency should be fast

swept, which is challenging because it is difficult to establish a stable oscillation from the thermal noise at a new frequency in a very short time. Non-stationary OEO sweeping would result in a temporally varying energy distribution between multiple eigenmodes of the OEO cavity, and hence cause degraded performance such as linewidth broadening and phase discontinuity. Fortunately, the FDML OEO can break the limitation of mode building time by matching the temporal period of the LCMW with the round-trip time delay of the OEO cavity. In this case, a new optoelectronic oscillation is established from a quasi-stationary mode, making it possible for an OEO to achieve fast and stable frequency scanning. In an FDML OEO, a microwave filter with fast frequency tunability is of great importance to generate LCMWs. In [10], a tunable microwave photonic filter by phase modulation (PM) to intensity modulation (IM) conversion is implemented using a wavelength tunable laser diode and a phase-shifted fiber Bragg grating (PS-FBG). Besides, period one dynamics of an optically injected semiconductor laser has also been applied to achieve fast frequency sweeping in an FDML OEO [12]. Based on the two schemes, LCMWs with a bandwidth as large as 7 GHz have been successfully generated. While, since the frequency scanning in both of the two systems are realized by dynamically varying the behavior inside a laser cavity, there are potential problems degrading the quality of the obtained LCMWs. For example, the spontaneous emission noise of the semiconductor laser leads to a large linewidth of each spectral tone of the generated LCMW [12], which degrades the phase coherence between adjacent pulses. In addition, the nonlinearity between the controlling signal and the output frequency in both of the two schemes causes a poor frequency modulation linearity of the LCMW. Compensation of such nonlinearity would complex the system and deteriorate the tunability.

In this letter, a stimulated Brillouin scattering (SBS)-based FDML OEO is proposed to generate broadband LCMWs. By applying a frequency sweeping optical carrier generated through high-order nonlinear electro-optical modulation, the pass band of the SBS-based microwave photonic filter can be tuned rapidly, and the obtained LCMW has a large bandwidth that is multiplied compared with the input frequency sweeping signal. This system makes the most of current electrical signal generators with high precision and great flexibility, and the SBS-based microwave photonic filter with narrow pass-band and fast response. Besides, the system uses a single laser source to generate both the pump light and the fast-swept probe light, which guarantees frequency-stable LCMW generation. Furthermore, the generated LCMW has a good frequency modulation linearity, and the bandwidth, duty

Manuscript received May 8, 2020; revised June 24, 2020; accepted July 20, 2020. Date of publication July 23, 2020; date of current version July 31, 2020. This work was supported in part by the NSFC Program under Grant 61871214, in part by the NSFC program of Jiangsu Province under Grant BK20180066, and in part by the Jiangsu Provincial Program for High-level Talents in Six Areas under Grant DZXX-005. (Corresponding authors: Fangzheng Zhang; Shilong Pan.)

The authors are with the Key Laboratory of Radar Imaging and Microwave Photonics, Ministry of Education, Nanjing University of Aeronautics and Astronautics, Nanjing 210016, China (e-mail: zhangfangzheng@nuaa.edu.cn; pans@nuaa.edu.cn).

Color versions of one or more of the figures in this letter are available online at <http://ieeexplore.ieee.org>.

Digital Object Identifier 10.1109/LPT.2020.3011411

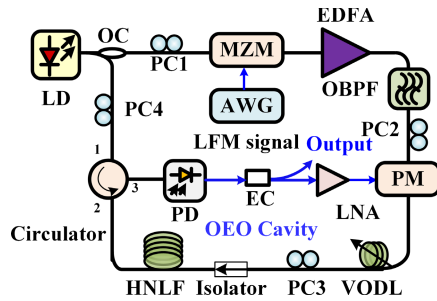


Fig. 1. Setup of the proposed LCMW generator. LD: laser diode; PC: polarization controller; OC: optical coupler; MZM: Mach-Zehnder modulator; OBPF: optical band-pass filter; PM: phase modulator; EDFA: erbium-doped fiber amplifier; PD: photodetector; EC: electrical coupler; LNA: low noise amplifier; VODL: variable optical delay liner; HNLf: highly nonlinear fiber.

cycle, and repetition rate can be tuned by simply setting the parameters of the low speed electrical signal generator.

II. PRINCIPLE

Fig. 1 shows the setup of the proposed photonic LCMW waveform generator. The light source from a laser diode (LD) having a frequency of f_{LD} is divided into two branches by an optical coupler (OC). The light in the upper branch passes through a polarization controller (PC: PC1) before sent to a Mach-Zehnder modulator (MZM), which is driven by a linearly frequency modulated (LFM) signal generated by a low-speed electrical arbitrary waveform generator (AWG). The MZM is properly biased and the LFM signal is set to have a large power to stimulate nonlinear electro-optical modulation. After the MZM, an erbium-doped fiber amplifier (EDFA) is used to boost the optical power and an optical bandpass filter (OBPF) is followed to select the $+n^{\text{th}}$ -order (n is a positive integer larger than 1) modulation sideband at $f_{LD} + nf_{LFM}$, in which $f_{LFM} = f_0 + kt$ ($0 \leq t \leq T_0$) is the instantaneous frequency of the LFM signal and T_0 is the frequency sweeping duration. The obtained optical signal acts as a frequency sweeping optical carrier, which passes through a PC (PC2), a phase modulator (PM), a variable optical delay line (VODL), a PC (PC3), an isolator (ISO), a span of highly nonlinear fiber (HNLf) and an optical circulator, respectively. Meanwhile, the optical signal from the lower branch of the OC is passed through a PC (PC4) and injected to the HNLf via the circulator. This optical signal travels in a counter propagating direction compared with the phase modulated optical signal, serving as the Brillouin pump. In the HNLf, the SBS effect leads to a Brillouin gain at the frequency of $f_{LD} - f_B$, with f_B being the Brillouin frequency shift. When the -1^{st} -order sideband of the phase modulated signal falls into the Brillouin gain region, i.e., the frequency of the signal driving the PM is $nf_{LFM} + f_B$, the power imbalance between the $\pm 1^{\text{st}}$ -order phase modulation sidebands leads to PM-to-IM conversion, and an RF signal at $nf_{LFM} + f_B$ is generated when the optical signal from port 3 of the circulator is sent to a photodetector (PD). In this process, the phase modulation combined with the SBS effect function as a tunable microwave photonic filter. To close the OEO loop, the electrical signal from the PD is amplified by a low noise amplifier (LNA) and applied to drive the PM. The oscillation frequency of this OEO can be tuned in the range from $nf_0 + f_B$ to $nf_0 + nkT_0 + f_B$. To generate the required LCMW, fast and stable tuning of the oscillation frequency of the OEO should be guaranteed. To this end, according to the

principle of an FMDL OEO, the temporal period of the input LFM signal (T) should be matched with the round-trip time delay of the OEO loop (τ), i.e., $\tau = \alpha T$ should be satisfied (α is a positive integer, named as the FDML factor in our study). This can be realized by jointly adjusting the VODL inside the OEO loop and properly setting the temporal period of the LFM signal. It should be noted that, T equals to T_0 only when the input LFM signal has a full duty cycle. The generated LCMW by the FDML OEO can be extracted to get the output signal using an electrical coupler (EC) after the PD. It should be mentioned that, four PCs are used in the system, among which PC1 and PC2 make sure the maximum modulation efficiency at the MZM and the PM, while PC3 and PC4 can adjust the polarizations of the pump and probe lights to guarantee a high SBS gain.

The advantages of the proposed scheme are summarized as follows. First, the frequency of the generated LCMW is multiplied by a factor of n and up-converted by f_B compared with the input electrical frequency sweeping signal. Thus, the generated LCMW not only has a broad bandwidth, but also has a good frequency modulation linearity originated from the input LFM signal. In addition, the bandwidth, central frequency, duty cycle and repetition rate of the obtained LCMWs is tunable. They can be easily adjusted by tuning the parameters of the electrical AWG. Furthermore, the SBS-based microwave photonic filter has a narrow pass band of tens of megahertz and a fast response in several nanoseconds [15], which is helpful to generate high-quality and fast frequency-swept LCMWs.

III. EXPERIMENT

An experiment based on the setup in Fig. 1 is carried out. In the experiment, the light source at 1550 nm generated by the LD (TeraXion) has a power of 16 dBm and a linewidth less than 12 kHz. The PM has a bandwidth of 40 GHz and a half wave voltage of 6 V. The PD (Optilab) has a 3-dB bandwidth of 30 GHz and a responsivity of 0.85 A/W. The LNA (XCLNA-19-31) works in the frequency range of 19-31GHz with a gain of 40 dB. The OBPF (Yenista Optics XTM-50) has an adjustable bandwidth with a 60-dB rejection ratio and a 500-dB/nm roll-off factor. The MZM (FTM7938EZ) is biased at the maximum transmission point to generate a signal mainly containing the optical carrier and the $\pm 2^{\text{nd}}$ -order sidebands ($n = 2$). The OBPF is used to select the $+2^{\text{nd}}$ -order sideband. Thus, the generated LCMW has a doubled bandwidth compared to that of the input LFM signal. The electrical spectrum is measured by an electrical spectrum analyzer (ESA: R&S FSV) and the generated LCMW is recorded by a real-time oscilloscope (Keysight DSO-X92504A) with a sampling rate of 80 GSa/s. The HNLf has a length of ~ 1 km and a nonlinear coefficient of $\sim 11 \text{ W}^{-1}\text{km}^{-1}$, and its Brillouin frequency shift is measured to be 9.4 GHz. The Brillouin threshold is estimated to be about 8 dBm, and the pump power launched into the HNLf is about 12 dBm, which ensures a high SBS gain. The total length of the OEO loop is about 1.07 km, corresponding to a round-trip time delay of $5.34 \mu\text{s}$, which is measured by a vector network analyzer (VNA, R&S ZVA 67).

First, the frequency response of the SBS-based microwave photonic filter is measured with the OEO loop opened. This

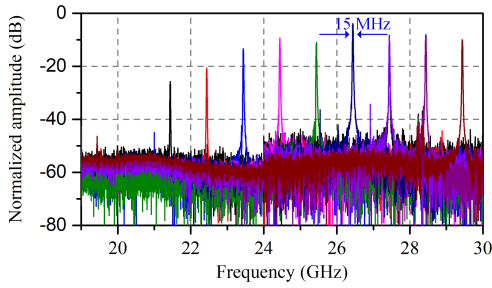


Fig. 2. Normalized frequency responses of the SBS-based microwave photonic filter with its central frequency tuned from 21.4 GHz to 29.4 GHz.

is implemented by driving the MZM with a single-tone RF signal, and recording the output amplitude response with a VNA by sweeping the frequency of the signal applied to the PM. Fig. 2 shows the normalized frequency responses of the SBS-based microwave photonic filter when the frequency of the signal applied to the MZM changes from 6 GHz to 10 GHz with a step of 500 MHz. As shown in Fig. 2, the central frequency of the pass band varies from 21.4 GHz to 29.4 GHz, with a step of 1 GHz. The 3-dB bandwidth of the pass band is measured to be 15 MHz, which is much narrower than the microwave photonic filter based on a PS-FBG (90 MHz) [7].

Then, performance of the LCMW generation by established FDML OEO is investigated. Considering the possible operation bandwidth determined by the available devices, the input LFM signal generated by the AWG (Keysight, M8195A) is set to have a central frequency of 8 GHz and a bandwidth of 2 GHz (7-9 GHz). It has a temporal period of $T = 5.34 \mu\text{s}$ with a duty cycle of 50%, indicating the frequency sweeping duration T_0 is $2.67 \mu\text{s}$ and the FDML factor α is 1. Fig. 3(a) shows the measured waveform of the generated LCMW in a single period. Its instantaneous frequency is calculated by performing short time Fourier transformation, with the result shown in Fig. 3(b). As shown in Figs. 3(a) and (b), the LCMW has a duty cycle of 50%, and it has a good frequency modulation linearity covering a bandwidth of 4 GHz (from 23.4 GHz to 27.4 GHz). Therefore, the signal frequency is successfully doubled and up-converted by 9.4 GHz compared to the input LFM signal. Fig. 3(c) shows the electrical spectrum of the generated LCMW, in which the out of band signal-to-noise ratio reaches 35 dB. To test the pulse compression property, autocorrelation of the generated LCMW is calculated, as shown in Fig. 3(d), where the full width at half maximum (FWHM) of the autocorrelation peak is 0.85 ns. The corresponding pulse compression ratio is 12560, which is close the TBWP (time bandwidth product) of the generated LCMW ($nkT_0^2 = 10680$).

For the proposed system, the duty cycle, frequency and bandwidth of the generated LCMW can be adjusted by changing the parameters of the input LFM signal. To show this property, Fig. 4 shows the waveforms and instantaneous frequencies of the LCMWs with a duty cycle of 25% and 90%, respectively, in which the bandwidth remains 4 GHz (23.4-27.4 GHz). Similarly, the bandwidth of the generated LCMWs can be tuned by changing the bandwidth of the input LFM signal. In the experiment, when the bandwidth of the input LFM signal centered at 8 GHz is tuned to 0.1 GHz, 1 GHz and 4 GHz, respectively, the waveforms and instantaneous frequencies of the generated LCMWs with a duty cycle

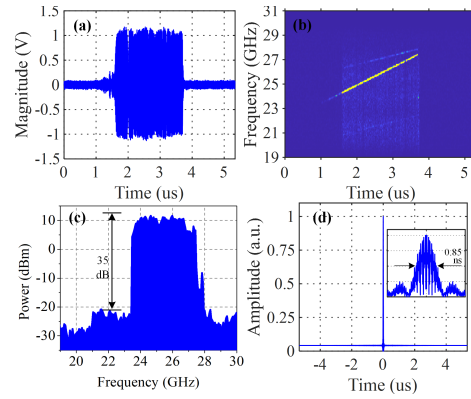


Fig. 3. (a) Waveform, (b) instantaneous frequency, (c) spectrum and (d) autocorrelation of the generated LCMW from 23.4 GHz to 27.4 GHz.

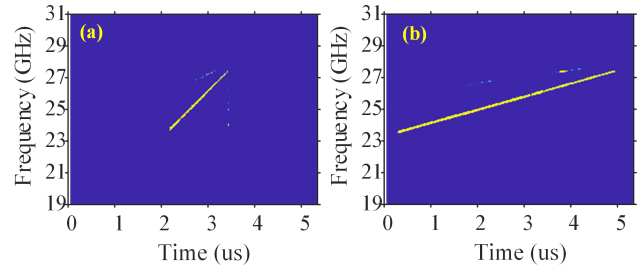


Fig. 4. Instantaneous frequencies of the LCMWs with duty cycle of 25% and 90%, respectively.

of 50% are shown in Fig. 5. As can be seen from Fig. 5, the bandwidth of the generated LCMW is 0.2 GHz, 2 GHz and 8 GHz, respectively. Fig. 6 shows that the frequencies of the LCMWs can also be tuned. It should be noted that, due to the limited bandwidths of the PD, and LNA in the experiment, the generation of LCMWs in other frequency bands is not demonstrated. Meanwhile, considering the interference of adjacent sideband, the OBPF is used to select other sideband such as $+1^{\text{st}}$ -order sideband, to generate the LCMW signals in lower frequency band. Without these limitations, LCMWs having a larger bandwidth at other frequency bands can be generated. Besides, the bandwidth and frequency can be further increased by choosing a higher-order ($n > 2$) modulation sideband generated by the MZM.

The repetition rate of the generated LCMW is determined by the temporal period (T) of the input LFM signal, which is closely related to the round-trip time delay of the OEO (τ) and the FDML factor (α). Usually, the time delay provided by a commercial VODL is limited and the length of the OEO cavity is hard to be tuned rapidly. Thus, to generate LCMW with different repetition rate, it is more practical and convenient to change the temporal period of the input LFM signal. Fig. 7 shows the instantaneous frequencies of the generated LCMWs when the temporal period of the input LFM signal is tuned to $2.67 \mu\text{s}$ and $1.07 \mu\text{s}$, and the corresponding FDML factor is 2 and 5, respectively. The duty cycles of the obtained LCMWs are all set to 90% and the signal bandwidths are 4 GHz. The repetition of the LCMWs in Fig. 7 is 373.8 kHz and 934.6 kHz, respectively. While changing the repetition rate, it is also found that the LCMWs remains a good frequency modulation linearity.

To investigate the tunability of the FDML OEO, the center frequency and scanning bandwidth of the LCMW can be tuned

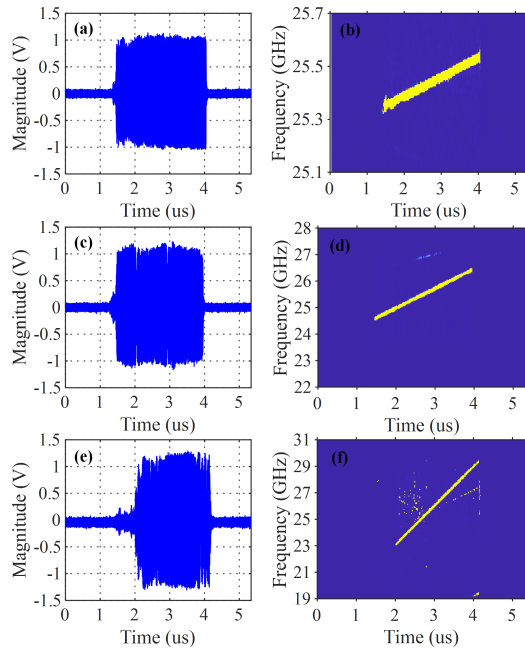


Fig. 5. (a), (c) and (e): The measured waveforms of the 50%-duty-cycle LCMWs with an input bandwidth of 0.2 GHz, 1 GHz and 4 GHz, respectively. (b), (d) and (f): The recovered instantaneous frequencies corresponding to the (a), (c) and (e), respectively.

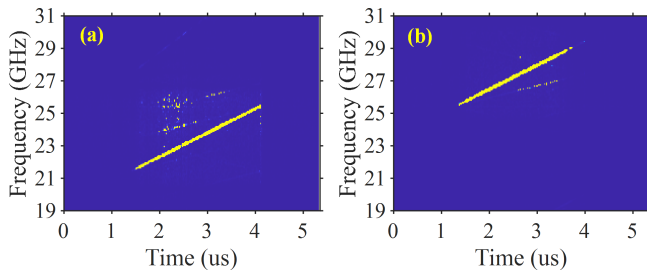


Fig. 6. The instantaneous frequencies of the generated LCMWs of the 50%-duty-cycle LCMWs with different central frequencies of 7GHz and 9GHz.

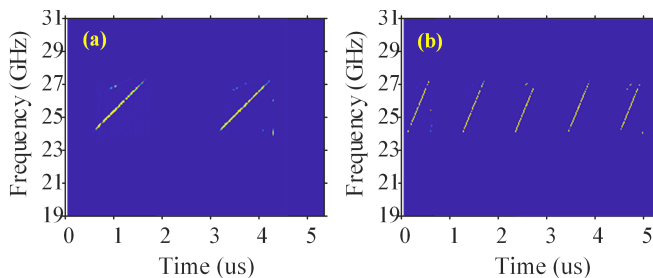


Fig. 7. The instantaneous frequencies of the generated LCMWs with different repetition rates (the corresponding FDML factors are 2 and 5).

based on the adjustment of the driving signal. As shown in Fig. 5, the scanning bandwidth changes from 0.2 GHz, 2 GHz, to 8 GHz. The TBWP keeps as high as 21360, which is competitive compared with traditional electrical signal generation schemes. Meanwhile, the linearity of the LCMW behaves well as the bandwidth increases in Fig. 5, which indicates fantastic tunability in bandwidth. The TBWP can be further extended by incorporating a longer cavity delay in the OEO

loop, which would ensure a longer time duration and larger scanning bandwidth of the generated LCMW. The frequency tuning range of the proposed OEO is determined by the frequency response of the optoelectronic devices used in the OEO's cavity. A larger tuning range can be obtained by using an LNA with broader bandwidth. An electrical band pass filter (EBPF) can be applied to eliminate the spurious generated due to the residual modulation sideband which fails to be completely suppressed.

IV. CONCLUSION

We have proposed and demonstrated a new method to generate LCMWs with an FDML OEO, which is realized applying a frequency-swept optical carrier generated by nonlinear electro-optical modulation and an SBS-based narrow-band tunable microwave photonic filter. Through experimental investigation, the proposed system is proved to have the capability to generate broadband LCMWs with tunable bandwidth, central frequency, duty cycle and repetition rate. As the rapid development of integrated microwave photonic techniques, and also encouraged by the numerous on-chip SBS-based signal processors, compact implementation of the proposed system is feasible. Thus, it has great potential to be applied in practical radar applications.

REFERENCES

- [1] M. I. Skolnik, *Radar Handbook*, 2nd ed. New York, NY, USA: McGraw-Hill, 1990.
- [2] D. R. Wehner, *High Resolution Radar*. Norwood, MA, USA: Artech House, 1987, p. 484.
- [3] F. Zhang, Q. Guo, and S. Pan, "Photonics-based real-time ultra-high-range-resolution radar with broadband signal generation and processing," *Sci. Rep.*, vol. 7, no. 1, p. 13848, Oct. 2017.
- [4] M. I. Skolnik, *Introduction to Radar Systems*. New York, NY, USA: McGraw-Hill, 1980, p. 590.
- [5] D. E. Leaird and A. M. Weiner, "Femtosecond optical packet generation by a direct space-to-time pulse shaper," *Opt. Lett.*, vol. 24, no. 12, pp. 853–855, 1999.
- [6] M. H. Khan *et al.*, "Ultrabroad-bandwidth arbitrary radiofrequency waveform generation with a silicon photonic chip-based spectral shaper," *Nature Photon.*, vol. 4, no. 2, p. 117, 2010.
- [7] J. Chou, Y. Han, and B. Jalali, "Adaptive RF-photonic arbitrary waveform generator," *IEEE Photon. Technol. Lett.*, vol. 15, no. 4, pp. 581–583, Apr. 2003.
- [8] P. Zhou, F. Zhang, Q. Guo, and S. Pan, "Linearly chirped microwave waveform generation with large time-bandwidth product by optically injected semiconductor laser," *Opt. Express*, vol. 24, no. 16, pp. 18460–18467, Aug. 2016.
- [9] F. Zhang *et al.*, "Photonics-based broadband radar for high-resolution and real-time inverse synthetic aperture imaging," *Opt. Express*, vol. 25, no. 14, pp. 16274–16281, Jul. 2017.
- [10] T. Hao *et al.*, "Breaking the limitation of mode building time in an optoelectronic oscillator," *Nature Commun.*, vol. 9, no. 1, p. 1839, May 2018.
- [11] T. Hao, J. Tang, W. Li, N. Zhu, and M. Li, "Tunable Fourier domain mode-locked optoelectronic oscillator using stimulated Brillouin scattering," *IEEE Photon. Technol. Lett.*, vol. 30, no. 21, pp. 1842–1845, Nov. 1, 2018.
- [12] P. Zhou, F. Zhang, and S. Pan, "Generation of linear frequency-modulated waveforms by a frequency-sweeping optoelectronic oscillator," *J. Lightw. Technol.*, vol. 36, no. 18, pp. 3927–3934, Sep. 15, 2018.
- [13] P. Zhou, F. Zhang, Q. Guo, and S. Pan, "Linear frequency-modulated waveform generation based on a tunable optoelectronic oscillator," in *Proc. Int. Topical Meeting Microw. Photon. (MWP)*, Oct. 2017, pp. 1–4.
- [14] X. S. Yao and L. Maleki, "Optoelectronic microwave oscillator," *J. Opt. Soc. Amer. B*, vol. 13, no. 8, pp. 1725–1735, 1996.
- [15] V. Kalosha, E. Ponomarev, L. Chen, and X. Bao, "How to obtain high spectral resolution of SBS-based distributed sensing by using nanosecond pulses," *Opt. Express*, vol. 14, no. 6, pp. 2071–2078, 2006.